IOPscience iopscience.iop.org

Home Search Collections Journals About Contact us My IOPscience

On the field-dependent magnetic structures of $CsCuCl_3$

This article has been downloaded from IOPscience. Please scroll down to see the full text article.

1994 J. Phys.: Condens. Matter 6 10105

(http://iopscience.iop.org/0953-8984/6/46/026)

View the table of contents for this issue, or go to the journal homepage for more

Download details:
IP Address: 171.66.16.151
The article was downloaded on 12/05/2010 at 21:08

Please note that terms and conditions apply.

J. Phys.: Condens. Matter 6 (1994) 10105–10119. Printed in the UK

On the field-dependent magnetic structures of $CsCuCl_3$

U Schotte†§, N Stüsser†, K D Schotte‡, H Weinfurter†||, H M Mayer† and M Winkelmann†

† Hahn-Meitner-Institut, Berlin Neutron Scattering Centre, 14109 Berlin, Germany
‡ Institut für Theoretische Physik, Freie Universität Berlin, 14195 Berlin, Germany

Received 16 March 1994, in final form 12 July 1994

Abstract. Neutron diffraction results on single crystals of $CsCuCl_3$ in high magnetic fields are reported. The fields were applied parallel (up to about 6.5 T) and perpendicular (up to 8.5 T) to the c axis of the hexagonal crystal. For the parallel field a spin-flop-like change in the magnetic structure at fields above 5.6 T was observed close below the Néel temperature. The magnetic phase diagram has been determined in the temperature range between 9.6 K and $T_N = 10.675$ K. In the perpendicular field the magnetic satellite reflections, originating from the helical magnetic spin structure of the Cu ions, shift their positions in rising field, indicating a stretching out of the helices. The results are interpreted in the light of recent theoretical predictions about the transitions being triggered by quantum or thermal fluctuations. In addition to determining the spin structures, we find that the critical exponent β is close to 0.25 in the low-field phase and probably close to 0.125 in the high-field phase.

1. Introduction

$CsCuCl_3$ is one of the widely investigated hexagonal perovskites consisting of chains of face-sharing octahedra along c, with the magnetic ions on the c axis interacting via superexchange, and well known for either quasi-1D magnetic properties or as 2D model candidates for a variety of interesting ordered states on the triangular lattice. $CsCuCl_3$, however, differs in that it is a cooperative Jahn–Teller system with chains of elongated octahedra of $CuCl_6$ arranged as spirals along the c axis, i.e. long axes never meet at the same anion (Schlueter *et al* 1966). This implies the lack of inversion symmetry, so that for the magnetic structure the Dzyaloshinsky–Moriya (DM) interaction along the chains has to be considered in addition to strong ferromagnetic exchange. The DM interaction tries to spread the spins apart and also acts like an easy-plane anisotropy, which otherwise for spin-1/2 systems like Cu is not relevant.

Neutron scattering below the ordering temperature of $T_N = 10.7$ K in zero magnetic field showed magnetic satellite reflections at $k = (n/3, n/3, l \pm \delta)$, but no intensity at $k = (n/3, n/3, l)$, where $n/3 = h \pm \frac{1}{3}$, $h = 0, 1, 2, \ldots$ and $l = 0, 6, 12, \ldots$. This has been interpreted as caused by antiferromagnetic triangular order in the ab plane and incommensurate magnetic spirals along the c axis with a pitch of about 5° (Adachi *et al* 1980).

In detail the interactions are even more complicated: electron spin resonance (ESR) modes measured with the external field H parallel to the c axis could be calculated

§ Also at Institut für Mineralogie, Universität Kiel, Kiel, Germany.
|| Now at Department of Physics, Universität Innsbruck, Innsbruck, Austria.

0953-8984/94/4610105+15$19.50 © 1994 IOP Publishing Ltd

satisfactorily only if in addition anisotropic exchange along c was assumed (Tanaka *et al* 1992). From the exchange parameters found, $CsCuCl_3$ is neither a quasi-1D nor a quasi-2D system; the ratio of the intra- to interchain exchange is about 6.

The most interesting finding in recent years has been the evidence of phase transitions of the magnetic structure in strong external magnetic fields (Nojiri *et al* 1988, Fedoseeva *et al* 1985, Gekht *et al* 1989). In the magnetization, anomalies have been seen at 1.1 K near 12 T: Noriji *et al* found a small vertical step in M versus H for H parallel to c, which points to a sudden flop-like change, while for H in the ab plane they found a short plateau indicating a smooth phase transition.

Using high pulsed magnetic fields parallel to c up to 14 T with a pulsed neutron source, new magnetic reflections have been observed (Mino *et al* 1993).

Also the ESR modes point to a qualitatively different magnetic order in this field region, and quite a few additional (weaker) resonances in the critical field region, with H in the ab plane, have been found, which have not yet been explained (Palme *et al* 1990, 1993, Ohta *et al* 1993, 1994).

Nuclear magnetic resonance (NMR) experiments (LeDang *et al* 1977) have shown no hint of the incommensurate spiral, but seem to point to a strictly hexagonal structure. The reason has remained obscure.

To date, quite detailed theoretical predictions about the magnetically ordered states in the field and the role of quantum and thermal fluctuations have been developed (Nikuni and Shiba 1993, Jacobs *et al* 1993, Rastelli and Tassi 1994). In this study we have used magnetic neutron diffraction to check some of these predictions. It is expected that the critical field for the spin-flop-like transition decreases as the temperature increases to the Néel temperature T_N from below. Therefore, we would expect to observe the transitions and deduce the associated spin structures even at fields up to about 8 T.

2. Theory and its implications for neutron diffraction

The energy of the spin system contains the ferromagnetic exchange J_0 along the chains, including a small anisotropy η, the antiferromagnetic exchange J_1 between the chains, the DM interaction (interaction vector $\boldsymbol{D}$) and the Zeeman energy:

$$H = -2J_0 \sum_{in} [\boldsymbol{S}_{in} \cdot \boldsymbol{S}_{in+1} + \eta(S^x_{in} S^x_{in+1} + S^y_{in} S^y_{in+1})] + J_1 \sum_{ijn} \boldsymbol{S}_{in} \cdot \boldsymbol{S}_{jn} - \sum_{in} \boldsymbol{D} \cdot (\boldsymbol{S}_{in} \times \boldsymbol{S}_{in+1}) - g\mu_B H \sum_{in} S^z_{in} \tag{1}$$

where n numbers the spins along the chains, i and j number the chains. We consider the case with the external magnetic field parallel to the z axis taken as the c axis of the crystal.

For crystal symmetry reasons the vector $\boldsymbol{D}$ will be parallel to the c axis (at least on average), so that this term effectively tends to spread the spins apart, working against the ferromagnetic exchange and thus producing the incommensurate spiral. The exchange anisotropy η as well as the DM interaction effectively produce an easy-plane anisotropy. Both contributions, however, lead to a relatively small anisotropy. These facts have led Nikuni and Shiba to consider fluctuations as a source for the triggering of the spin-flop transition.

The Hamiltonian H, even in the classical limit, is too complicated to be of direct use for the analysis of neutron diffraction data. Using a coordinate transformation that rotates

the spins in the nth layer by n times the helical pitch in the xy plane, which does not affect the Zeeman term (Tanaka *et al* 1992), one obtains formally N identical triangular antiferromagnetic planes, so that we can drop the index n:

$$E_0/N = -2\tilde{J}_0 S^2 + \tfrac{2}{3}(\tilde{J}_0 - J_0)\sum_i^3 (S_i^z)^2 + 2J_1 \sum_i^3 \boldsymbol{S}_i \cdot \boldsymbol{S}_{i+1} - \tfrac{1}{3} g\mu_B H \sum_i^3 S_i^z. \tag{2}$$

The $\boldsymbol{S}_i$ now denote three sublattice spins of length S and

$$\tilde{J}_0 = J_0[(1+\eta)^2 + (D/2J_0)^2]^{1/2} \tag{3}$$

where D is the modulus of $\boldsymbol{D}$. D is of course responsible for the helical pitch:

$$Q = \tan^{-1}[D/2J_0(1+\eta)]. \tag{4}$$

For the parameters from Tanaka *et al* we take $J_0 = 28$ K, $J_1 = 4.9$ K and $\tilde{J}_0 - J_0 = 0.32$ K, close to those found earlier by Tazuke *et al* (1981).

Up to a constant, the energy can likewise be written as

$$\begin{aligned} E_0/N &= J_1(\boldsymbol{S}_1 + \boldsymbol{S}_2 + \boldsymbol{S}_3 - g\mu_B \boldsymbol{H}/6J_1)^2 + \Delta \sum (S_i^z)^2 \\ \Delta &= \tfrac{2}{3}(\tilde{J}_0 - J_0). \end{aligned} \tag{5}$$

Without the anisotropy term proportional to Δ, all ground-state configurations satisfying the condition

$$\boldsymbol{S}_1 + \boldsymbol{S}_2 + \boldsymbol{S}_3 = (g\mu_B/6J_1)\boldsymbol{H} \tag{6}$$

are degenerate. Only the anisotropy term decides which has the lowest energy. To first order in Δ, it is not necessary to minimize the full energy (5) since the squared bracket yields at least second-order contributions if the spin components have a Δ correction. At first sight the problem of finding the probable low-energy configurations fulfilling (6) seems trivial, since an easy-plane anisotropy favours a triangular structure flat in the ab plane; an applied field would pull up the spins parallel to the z axis so that they look like an 'umbrella' (see figure 1(a)).

However, as the Cu spin and the anisotropy are small, it has been recognized that, in a strong magnetic field, quantum and thermal fluctuations stabilize configurations that are planar with respect to the field rather than 'umbrella'-like (Kawamura 1984, Chubukov and Golosov 1991). According to Nikuni and Shiba, this causes the spin-flop transition noticed as the step in the magnetization found by Motokawa's group (Nojiri *et al* 1988). This gives a selection of spin configurations to be considered.

Mathematically, the degeneracy of the spin arrangements obeying condition (6) arises from the fact that (6) does not fix the spin components (or six angles) of a general configuration, since one has only three conditions: the sums of the x and y components have to be zero, and for the z components one has

$$\tilde{S}_1^z + \tilde{S}_2^z + \tilde{S}_3^z - 3h = 0 \qquad \text{with } h = H/H_s \text{ and } H_s = 18J_1 S/g\mu_B \tag{7}$$

where the angular part $(\tilde{S}_i^x, \tilde{S}_i^y, \tilde{S}_i^z)$ (= unit vector) and length S of the spin have been separated; the field of paramagnetic saturation H_s has been found near 32 T at about 1 K by Motokawa's group.

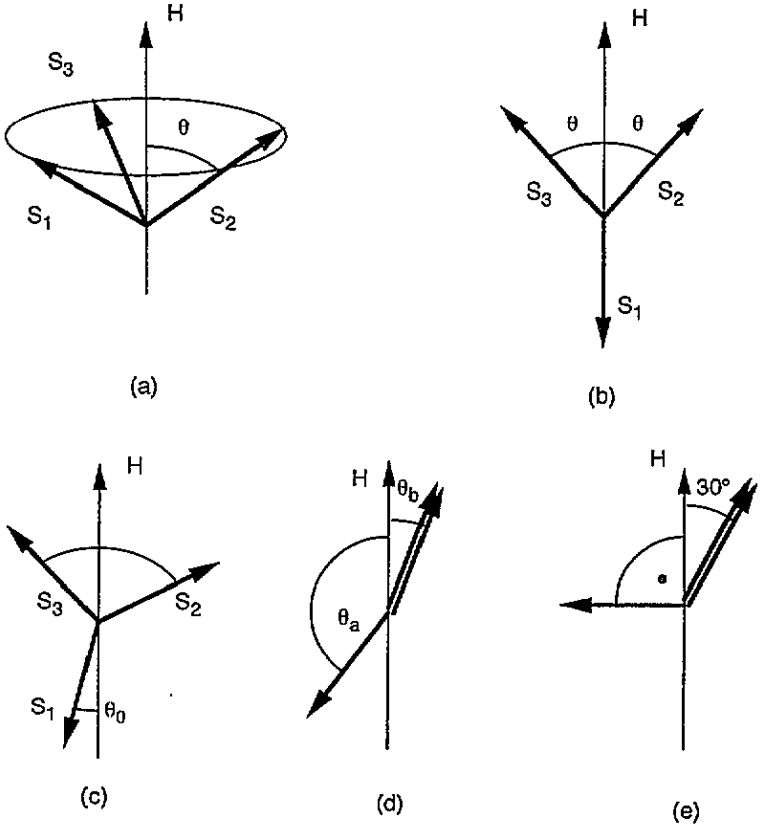

Figure 1. Sublattice spin configurations to be discussed, magnetic field H parallel to the $z = c$ axis: (a) 'umbrella' configuration; (b) coplanar configuration orthogonal to the ab plane; (c) general coplanar configuration with θ_0 as a variable; (d) collinear configuration; (e) special case of (d) referring to the energy minimum for easy-plane anisotropy.

At finite temperatures one sees that $S = S(T)$ should be proportional to the magnetization. Going over the free energy one has to subtract the entropy multiplied by the temperature from the energy E_0 in (2). Minimizing this free energy in mean-field approximation, one can first determine the temperature dependence of the sublattice magnetization $|S_i| = S(T)$ and then the orientations $\tilde{S}_i$ using (7) with a now temperature-dependent saturation field $H_s(T) = H_s S(T)$. The critical exponent for the magnetization β is of course 1/2 in this approximation. For our experiments close to the Néel temperature β is expected to be smaller. For the interpretation of the results β plays the role of a fitting parameter.

For the high-symmetry configurations, proposed above and shown in figure 1, namely the 'umbrella' and planar configurations, the dependence of the components, especially the z components, on the field and their stability ranges are easily found from the above conditions (see table 1). The general coplanar configuration with $0 \leqslant \theta_0 < 60°$ (figure 1(c)) has a limit of stability between $h = 1/3$ and $h = 1$.

By using table 1 to calculate the anisotropy term of (5), one finds that the 'umbrella' configuration has the lowest energy and that a collinear configuration always has a higher energy than any coplanar configuration. It may be demonstrated that this holds for all θ_0. The collinear configuration has a minimum for the angles of figure 1(e).

Table 1. The z components of spin configurations discussed, from figure 1, and their stability ranges in the field $h = H/H_s$ defined in (7).

Configuration	Spin angles in field h	Stability range
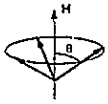	$\tilde{S}_i^z = \cos\theta = h$	$-1 \leqslant h \leqslant 1$
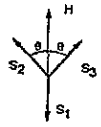	$\tilde{S}_1^z = -1$ $\tilde{S}_2^z = \tilde{S}_3^z = \cos\theta = \frac{1}{2}(3h+1)$	$-1 \leqslant h \leqslant \frac{1}{3}$
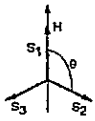	$\tilde{S}_1^z = 1$ $\tilde{S}_2^z = \tilde{S}_3^z = \cos\theta = \frac{1}{2}(3h-1)$	$-\frac{1}{3} \leqslant h \leqslant 1$
	$\tilde{S}_1^z = \cos\theta_a = \frac{3}{2}h - 1/(2h)$ $\tilde{S}_2^z = \tilde{S}_3^z = \cos\theta_b = \frac{3}{4}h + 1/(4h)$	$\frac{1}{3} \leqslant h \leqslant 1$

It has been found that thermal fluctuations favour the opposite: according to Kawamura (1984), in the presence of the magnetic field they contribute a term to the free energy that is proportional to J_1 and contains the *product* of the z components of the spin configurations (instead of the sum of the squares). Using such a three-spin term one finds from table 1 that the 'S_1 down' and, beyond its stability limit of $h = 1/3$, the collinear configuration have the lowest energy. Kawamura's result seems to be limited to the planar rotator model on the triangular lattice. The 2D Heisenberg case gives, however, conflicting results (Miyashita 1986).

Nikuni and Shiba undertook the more difficult 3D calculation of quantum fluctuations and thermal fluctuations from the spin waves, and arrived at basically the same result as Kawamura (1984). According to their theory, at $T = 0$ a first-order phase transition takes place at $h_c = 1/3$ because the umbrella structure flips over into a coplanar, probably the collinear, configuration.

If the external magnetic field is applied in the ab plane the coordinate transformation from above cannot be applied and analytically the problem becomes intractable. As to the phase transition, field and spins are already in coplanar configuration with different angles θ_0. They turn into the collinear configuration at their appropriate $h_c(\theta_0)$ values. For antiferromagnetically coupled stacked triangular lattices, it seems that these are smooth transitions (see for example Plumer and Caillé 1990). Also the strong ferromagnetic and the DM interactions along the chain could make the global transition process look smooth. Eventually, for $H \to H_s$, all spins have to turn parallel to the field and the helicity will disappear.

Some results of approximate and numerical treatments by Jacobs *et al* (1993) can be plausibly understood, and will be used in the discussion of the experiments. These authors predict a second-order phase transition.

With regard to diffraction experiments, all magnetic configurations discussed involve the tripling of the chemical cell due to antiferromagnetic order in the ab plane. Together with the helical spin order along the c axis this gives reflections ('satellites') at $(n/3, n/3, l \pm \delta)$

with $n/3 = h \pm \frac{1}{3}$. All configurations fulfilling (6) have a ferromagnetic component along c in non-zero field, which adds intensity only at positions of nuclear reflections, while the planar arrangements, figures 1(*b*) to (*e*), give additional reflections at $(n/3, n/3, l)$. The appearance of these extra peaks signals the onset of the new phase.

If the field is in the *ab* plane one can anticipate that, when the helicity disappears, the 'satellites' merge to give peaks at $(h \pm \frac{1}{3}, h + \frac{1}{3}, l)$.

The explicit magnetic structure factors F_{m}^2 for a general scattering vector and all relevant configurations are given in the appendix. For helical spin ordering they may be written in the form

$$F_{\mathrm{m}}^2 = S^2 f \sum_{\tau} \{I_1 \delta(k - \tau) + I_2[\delta(k + Q - \tau) + \delta(k - Q - \tau)]\}$$
$$f = (2\pi)^3 N_{\mathrm{m}} / V_{0\mathrm{m}} \tag{8}$$

where τ is a reciprocal lattice vector, N_{m} and $V_{0\mathrm{m}}$ are number and volume of the magnetic unit cells.

The part containing the spiral vector Q refers to the 'satellites' at $(n/3, n/3, l \pm \delta)$, I_2, while the other part I_1 refers to the ferromagnetic contribution due to the field at (hhl) and to the new reflections at $(n/3, n/3, l)$ for the coplanar and collinear configurations.

I_1 and I_2 can be expressed by the characteristic angles θ, θ_{a} and θ_{b} and thereby as a function of h with table 1. In the following we can omit the subscripts 1 and 2 by indicating the Bragg indices.

The magnetic contribution to the nuclear Bragg peaks is the same for all configurations, and it is proportional to

$$I(hhl) = (1 - \tilde{k}_z^2)(3Sh)^2. \tag{9}$$

The intensity of the satellites from the umbrella configuration is proportional to

$$I_{\mathrm{umb}}(n/3, n/3, l \pm \delta) = (1 + \tilde{k}_z^2) S^2 \tfrac{9}{8}(1 - h^2). \tag{10}$$

For the two typical coplanar configurations with 'S_1 up' and 'S_1 down' one has

$$I_{\mathrm{cop}}(n/3, n/3, l \pm \delta) = (1 + \tilde{k}_z^2) S^2 \tfrac{9}{16}(1 - 3h^2 \pm 2h) \tag{11}$$

with '+' for 'S_1 up' and

$$I_{\mathrm{cop}}(n/3, n/3, l) = (1 - \tilde{k}_z^2) S^2 \tfrac{9}{4}(1 \mp h)^2 \tag{12}$$

now with '−' for 'S_1 up', and finally for the collinear configuration one has

$$I_{\mathrm{col}}(n/3, n/3, l \pm \delta) = (1 + \tilde{k}_z^2) S^2 \tfrac{1}{4}\{[1 - (\tfrac{3}{2}h - 1/2h)^2]^{1/2} + [1 - (\tfrac{3}{4}h + 1/4h)^2]^{1/2}\} \tag{13}$$

and

$$I_{\mathrm{col}}(n/3, n/3, l) = (1 - \tilde{k}_z^2) S^2 \tfrac{9}{16}(h - 1/h)^2. \tag{14}$$

Thus in principle one can observe the magnetic phase transition in the rising field at fixed temperature below T_{N}.

The intensities (9) to (14) are shown in figure 2 for $\tilde{k}_z = 0$ (which is sufficient for the $l = 0$ reflections), choosing the 'S_1 up' type from the coplanar configurations, which remains stable up to saturation. Comparing figures 2(*a*) and (*b*), it seems that the collinear and the coplanar configurations are not easy to distinguish experimentally. It turns out, however, that an unambiguous distinction can be made when measuring the peak intensities at fixed field as a function of temperature: the intensities of 'satellite' and new 'central' reflection cross for the collinear configuration while those of the coplanar structure do not.

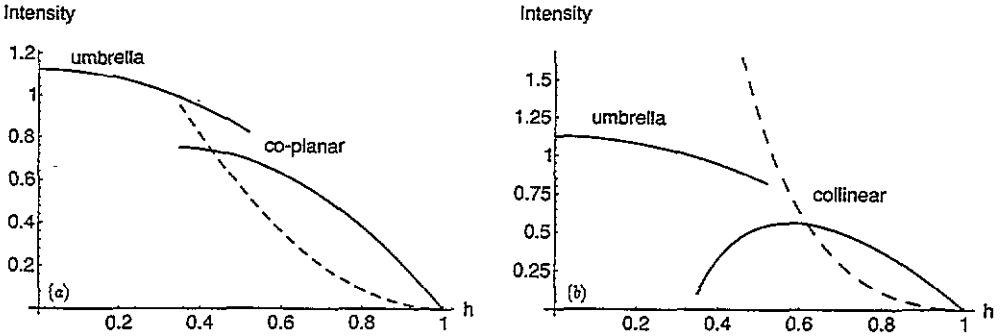

Figure 2. Predicted dependence of peak intensities on the magnetic field $h = H/H_s$: (*a*) for the 'umbrella' and coplanar configurations with 'S_1 up' from equations (10)–(12), and (*b*) for the 'umbrella' and collinear spin configurations from equations (10), (13) and (14) calculated for $\bar{k}_z = 0$, representative for typical reflections $(n/3, n/3, 0)$ (----) and $(n/3, n/3, 0\pm)$.

Table 2. Integrated intensities of magnetic satellite reflections measured at 4 K in zero magnetic field. The intensities are multiplied by the Lorentz factor $\sin(2\theta)$ and divided by the squared magnetic form factor f_m. The number in parentheses denotes the error due to the counting statistics as well as the uncertainty in the estimation of the background.

h	k	l	Intensity $\times \sin(2\theta)/f_m^2$
1/3	1/3	0+	12 580 (360)
1/3	1/3	0−	11 610 (340)
2/3	2/3	0+	8850 (275)
2/3	2/3	0−	8110 (250)
1/3	1/3	6+	22 720 (600)
1/3	1/3	6−	25 690 (670)
2/3	2/3	6+	23 750 (630)
2/3	2/3	6−	23 830 (630)

3. Experimental results and discussion

Different single crystals of $CsCuCl_3$ with volumes between 300 and 1000 mm^3 were studied by elastic neutron scattering at 2.4 Å using the diffractometers E4 and E6 of the BER II Research Reactor of the Hahn-Meitner-Institut, Berlin, and the TAS 6 at the Risø Research Rector in Denmark. All diffraction measurements were performed in the (hhl) zone because of the anticipated triangular spin ordering in the ab plane. Nuclear reflections were measured at room temperature. The observed structure factors agreed with the calculated ones, using the space group $P6_122$ and $a = 7.235(2)$ Å and $c = 18.242(4)$ Å for $CsCuCl_3$ (Schlueter *et al* 1966).

3.1. Zero-field measurements

Magnetic Bragg intensities were collected in the spin-ordered phase below 10.68 K. In agreement with the neutron diffraction results reported earlier by Adachi *et al* (1980), satellite reflections were observed at reciprocal lattice points $(n/3, n/3, l \pm 0.085)$ with $n = 1, 2$ and $l = 0, 6$. All observed intensities (table 2) agree well with a triangular antiferromagnetic ordering in the ab plane, thus tripling the chemical unit cell, and the spiralling of the magnetic moments along c with the spin rotation plane confined to the ab plane.

In addition to the satellite reflections, much weaker reflections of magnetic origin occurred at $(n/3, n/3, l \pm 0.085)$, with $l = 1, 2, 3, 4, 5$, the intensities of which change significantly with index l. They are strongest for $l = 1$ and 5. These reflections can be explained by the fact that the Cu ions are not placed precisely on the c axis, but are displaced, following the structural spiral, by a few tenths of an ångström ($u = 0.0616a$). The relative intensities are well described by the appropriate geometrical structure factor (Adachi *et al* 1980). Recently Mekata *et al* (1994) also measured these weaker satellites with the aim to find more information on deviations of the spin angles out of the ab plane.

In order to investigate the critical behaviour associated with the antiferromagnetic to paramagnetic phase transition, the integrated intensity of the (1/3, 1/3, 0.085) reflection was measured in the temperature range from 8 to 10.7 K (figure 3). Close to the Néel point the temperature dependence of the intensity can be expressed by

$$I \propto [(T_N - T)/T_N]^{2\beta} \equiv t^{2\beta} \tag{15}$$

where β denotes the critical exponent of the ordering parameter. Least-squares fits to the experimental data in the reduced temperature ranges $t < 2 \times 10^{-1}$, $t < 6 \times 10^{-2}$ and $t < 3.5 \times 10^{-2}$ yielded critical exponents $\beta = 0.25(2)$, 0.24(2) and 0.23(2), respectively. The Néel point was determined by all least-squares fits with a precision better than 10^{-2} K to be $T_N = 10.675$ K.

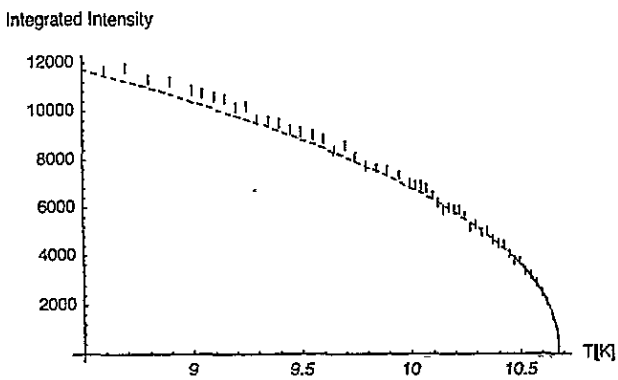

Figure 3. Peak intensity of (1/3, 1/3, 0.085) in zero field as a function of temperature, with statistical errors of the data indicated. The fitted function is proportional to $(T_N - T)^\beta$ with $T_N = 10.675$ K and $\beta = 0.25$ for $T \geqslant 10.475$ K, shown dashed beyond the fit region to show that it is acceptable also for lower temperatures.

3.2. Measurements in magnetic fields parallel to c

The temperature and magnetic field ranges studied in our experiments extended from 9 to 11 K and from zero up to fields of $H = 6.52$ T. The measurements were performed as temperature scans at different field strengths. Data were collected by ω scans around the reciprocal lattice points. Two regions with different types of magnetically ordered states could be identified by neutron diffraction. The first is characterized by the presence of the same 'satellite' reflections that were observed for the spin-ordered phase at zero field. In the second phase, closer to T_N, additional magnetic reflections appear at reciprocal lattice

points $(n/3, n/3, l)$, $n = h \pm \frac{1}{3}$, $l = 1, 6$. At the phase boundary a sudden decrease in intensity of the $(n/3, n/3, l \pm 0.085)$ reflections occurred, without change of their position, accompanied by the appearance of the $(n/3, n/3, l)$ reflections.

In figure 4 the measured portion of the phase diagram is shown. The lower curve is the boundary for the first-order transition; it should be taken as a guide for the eye.

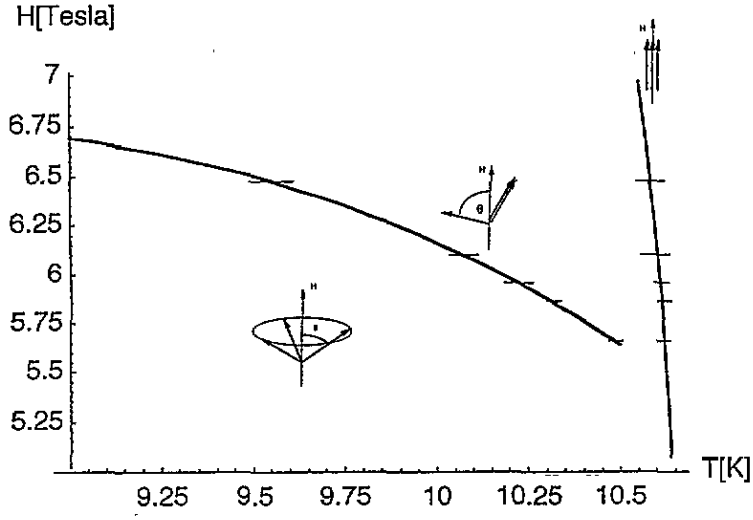

Figure 4. Phase diagram with the three observed phases indicated: 'umbrella', collinear and paramagnetically saturated state. The lower curve is the boundary for the first-order transition, and the upper curve follows const$(T_N - T)^\beta$, here for $\beta = 0.25$, but $\beta = 0.125$ would also give a fit within the error bars.

The upper curve for the second-order transition into the paramagnetically saturated state is fitted well by a $(1 - T/T_N)^\beta$ law. Within the error bars, $\beta = 0.125$ and 0.25 fit nearly equally well. For the figure 0.25 is used. Below 5.6 T no phase transition could be observed. A similar phase diagram has been found by Gekht *et al* (1989) with magnetization measurements. A different magnetic structure theory was used though.

For the interpretation of the peak intensities as a function of temperature, using (9) to (14), we need $h(T)$.

As discussed above, we assume that $S(T)$ follows (with $B = \text{const}$):

$$S(T) = B[(T_N - T)/T_N]^\beta. \tag{16}$$

Then from (7) we have

$$h(T) = (H/H_s B)[(T_N - T)/T_N]^{-\beta} \tag{17}$$

from which, by the way, the Néel temperature in the field $T_N(H)$ follows with the condition $h(T) = 1$ for $T = T_N(H)$:

$$T_N(H) = T_N - T_N(H/H_s B)^{1/\beta} = T_N - CH^2 \tag{18}$$

the latter for $\beta = 1/2$, as expected in molecular theory.

For our context, we chose a physically reasonable form of $h(T)$:

$$h(T)/h(T_c) = [(T_N - T)/(T_N - T_c)]^{-\beta} \tag{19}$$

with T_c the experimentally found critical temperature of the phase transition. $T_N(H)$ can also be determined from the experiment. Once β is found, then $h(T_c)$ is calculated from (19) and the angles of the configuration at the phase transition with table 1.

Now there is no obvious reason why in the transformed state the same critical exponent 0.25 as in zero field should prevail, especially since the coplanar and collinear configurations have no chirality, which might be the reason for the unusual value, as suggested by Mekata (private communication) following Kawamura (1991).

Figures 5(*a*) and (*b*) show how the exponent β is determined: the integrated intensities for the (1/3, 1/3, +0.085) and (1/3, 1/3, 0) reflections in $H = 6.52$ T are shown together with least-squares fits of (13) and (14) (collinear configuration) with $S(T)$ and $h(T)$ inserted, using $\beta = 0.125$, 0.25 and 0.36. (The prefactors of (13) and (14), containing also the unknown B from $S(T)$, are the fitting parameters.) For the (1/3, 1/3, 0) reflection obviously $\beta = 0.125$ gives the best fit; for the 'satellite' peak (1/3, 1/3, +0.085) this decision is not quite so obvious, and there only the Heisenberg value 0.36 can be excluded (figure 5(*b*)). Exactly the same conclusion was reached when treating in the same way the data sets for $H = 5.9$, 6 and 6.14 T.

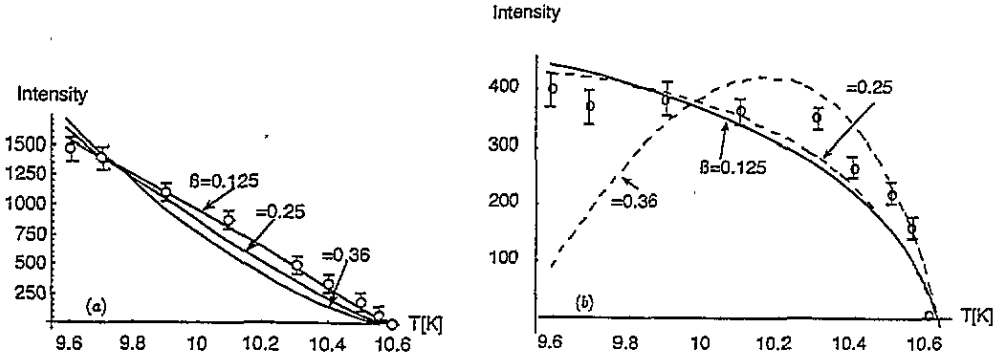

Figure 5. Peak intensities normalized to 10^5 monitor counts and multiplied by $\sin(2\theta)/f_m^2$ (see heading of table 2) of the (1/3, 1/3, 0) reflection (*a*) and the (1/3, 1/3, 0.085) reflection (*b*) as a function of temperature in a field of 6.52 T. Errors include uncertainties in the background determination and the counting statistics. Full curves are least-squares fits of (13) and (14) to the data using (16) and (17). Although it is less obvious from (*b*), a clear preference of $\beta = 0.125$ was deduced from (*a*).

In figure 6 results for $H = 5.9$ T are displayed together with the fitted theoretical curves for the collinear structure. Mostly data for (1/3, 1/3, ±0.085) and (1/3, 1/3, 0) are shown, and some error bars are shown to give an impression of their size. The calculations were performed for scattering vectors with $\bar{k}_z \simeq 0$; there are also a few data points and the calculated curves for $l = 6$ to make sure of the consistency of the structure determination. All efforts failed to fit the data using the structure factors for the coplanar configuration.

The intensity for the 'satellite' peaks below the phase transition is fitted using $\beta = 0.25$.

At all phase transitions observed we found $h(T_c) \geqslant 0.5$. The collinear structure then already strongly resembles figure 1(*e*). When approaching the region of the possible bicritical point as close as possible, the angle θ_a has only dropped to about 70°.

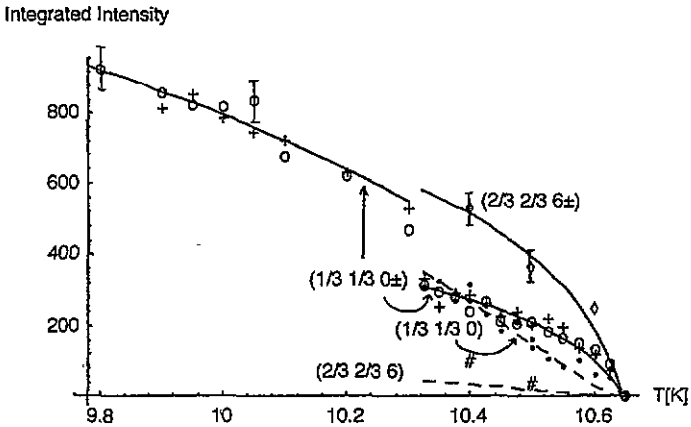

Figure 6. Peak intensities in the field of $H = 5.9$ T as a function of temperature calculated as for figure 5, now with $\beta = 0.125$ for the high-field phase and $\beta = 0.25$ for the 'umbrella' phase below 10.3 K. Only a few data for $l = 6$ are available, and they show the consistency of the spin structure determination.

3.3. Finite-field results for fields in the ab plane

We turn to the case with the crystal mounted in a magnet with vertical field, i.e. the field in the *ab* plane. These measurements were performed at the multidetector instrument E6 and at the single-detector instrument TAS 6. In the magnetically ordered phase a shift of the satellites along the l direction towards the $(h \pm \frac{1}{3}, h \pm \frac{1}{3}, l)$ points with increasing field strength was observed while the intensities remained unchanged as compared to the zero-field intensities. This indicates that in the region of temperatures and fields investigated the triangular spin ordering in the *ab* plane persists in the magnetic field.

In order to anticipate what happens in the case $H \perp c$, consider each antiferromagnetic plane characterized by the configuration in figure 1(*c*) (now looking down on the *ab* plane) with θ_0 proceeding by about 5° from plane to plane. The quantum and thermal fluctuations seem to act as a uniaxial anisotropy in the field direction, in the sense that the field favours the collinear configuration, which starts, on the low-field side at $h = 1/3$, with two spins parallel to H and one antiparallel. In high fields all three spins are more or less parallel to the field, but the intermediate arrangements must be complicated, as indicated by many unexplained extra ESR resonances found by Palme *et al* (1990, 1993) and by Ohta *et al* (1993, 1994).

The change in the spiral pitch in relatively low fields is shown in figure 7, together with the analytical result of Jacobs *et al* (1993), which fits well for fields below 4.5 T. The experiments were performed at 5 and 3.75 K, and for the figure we took $h = H/(30\ \mathrm{T})$. Also shown are extrapolations to indicate the end of the incommensurate phase. The transition seems to be near the value expected from numerical work by Jacobs *et al* near $h_c = 0.42$.

Obviously for these experiments the temperatures chosen were too low in relation to the available magnetic fields in order to observe the approach to the expected second-order phase transition.

Since the critical h_c values appear to be comparable to those for H parallel to c, neutron diffraction experiments similar to those for H parallel to c, at the highest available fields, within half a degree below T_N, are planned for the investigation of this phase transition.

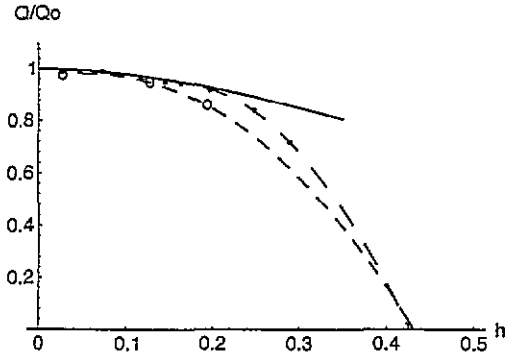

Figure 7. Dependence of the pitch of the helical spin chains along the c axis with the applied field in the ab plane, shown as a function of H/H_s with $H_s = 30$ T. The errors for Q/Q_0 are around 1%. The full curve is theoretically predicted for low fields, and the broken curves are polynomial fits as guides for the eyes.

4. Summary and conclusions

The aim to investigate the phase transition of $CsCuCl_3$ in a magnetic field and to check the new theory by Nikuni and Shiba (1993) and Jacobs *et al* (1993) has partly been reached.

In order to observe the spin-flop-like transition in the field parallel to the c axis where the magnetization $M(H)$ has a step-like behaviour at low temperatures and accordingly high fields, the diffraction measurements were performed close to the Néel temperature to make use of the lower fields available. We could prove that a transition from an 'umbrella' to a collinear phase takes place in accordance with the theoretical predictions. The transition temperature is so close to T_N that one can assume to be in the classical regime where thermal—not quantum—fluctuations are responsible for the preference of the collinear configuration, in spite of $CsCuCl_3$ having an easy-plane anisotropy.

Since the diffraction experiments were performed at constant field and varying temperature close to T_N, it was necessary to decide on and use the critical exponent β for the interpretation of the observed magnetic intensities. The question whether the critical exponent of 0.25 measured at zero field in accordance with the theoretical prediction for a chiral x–y model is also valid in the 'umbrella' phase at higher magnetic fields could be answered affirmatively. In this phase the antiferromagnetic order is still a planar one, stabilized by the planar anisotropy. This is irrespective of an additional magnetization in the z direction due to the magnetic field, and does not differ for the different magnetic sublattices. However, this situation changes for the collinear phase. We found that β should take the lower value of 0.125. Why this two-dimensional Ising value appears there is not clear. The experimental data were not quite sufficient for an unambiguous answer for the magnetic-field dependence of β, but the trends are certain.

The experiments for H in the ab plane were limited at low temperatures to the 'small' field region relatively far away from the expected phase transition with the helices straightened. It has been proved that the spiral pitch diminishes substantially if a strong magnetic field is applied in the ab plane. It should completely disappear where a shoulder had been found in the magnetization measurement $M(H)$, but these high fields could not be reached in our neutron diffraction experiments at relatively low temperatures.

It is planned to investigate this transition also close to the Néel temperature.

It now seems not evident that the shoulder found in the magnetization $M(H)$ for

H perpendicular to c must be at the same point as the step for H parallel to c for all temperatures.

Acknowledgments

We are grateful to H Shiba (Tokyo), M Motokawa (Sendai) and U Everts (Hannover) for valuable discussions. The experiments in Berlin benefited from technical and computational support by G Lampert, X Hu, M Meissner and F Wagemann. The crystals were provided by H A Graf and S Pfannenstiel. The use of the neutron scattering facilities at the Risø Research Reactor and the hospitality enjoyed there are gratefully acknowledged.

Appendix. Magnetic structure factors for the configurations of figure 1

Owing to antiferromagnetic ordering in the triangular lattice of the ab plane the chemical unit cell is tripled; we choose the lattice constants $a/\sqrt{3}$ and c and $\gamma = 60°$. Neglecting the small structural helix of the Cu ion positions, the magnetic moments are located at

$$\boldsymbol{d}_1 = 0 \qquad \boldsymbol{d}_2 = (1/3, 1/3, 0) \qquad \boldsymbol{d}_3 = 2\boldsymbol{d}_2. \tag{A1}$$

Then one has to calculate

$$F_{\mathrm{m}}^2 = \sum_{im} \sum_{ij} \sum_{\alpha\beta} (\delta_{\alpha\beta} - \tilde{k}_\alpha \tilde{k}_\beta) S_{li}^\alpha S_{mj}^\beta \exp[\mathrm{i}\boldsymbol{k} \cdot (\boldsymbol{l} + \boldsymbol{d}_i - \boldsymbol{m} - \boldsymbol{d}_j)] \tag{A2}$$

where $\boldsymbol{k}$ is the scattering vector ($\tilde{k}$ is normalized to unity), α and β denote Cartesian coordinates, $\boldsymbol{s}_{li}$ are the spin vectors of length S, and $\boldsymbol{l}$ and $\boldsymbol{m}$ stand for lattice cell vectors.

For all configurations shown in figure 1 the vectors of the spiralling spins can be written in the following form:

$$\boldsymbol{S}_{li} = S(\sin\vartheta_i \cos(\boldsymbol{Q} \cdot \boldsymbol{l} + \phi_i), \sin\vartheta_i \sin(\boldsymbol{Q} \cdot \boldsymbol{l} + \phi_i), \cos\vartheta_i). \tag{A3}$$

The vector $\boldsymbol{Q}$ describes the spiral along c; it is parallel to the c axis and its magnitude is the interplanar turn angle.

For the 'umbrella' one has

$$\vartheta_i = \theta \qquad \text{and} \qquad \phi_1 = 0 \qquad \phi_2 = 2\pi/3 \qquad \phi_3 = 4\pi/3.$$

For the 'S_1 up' configuration of figure 1(b) (or 'S_1 down') one has

$$\vartheta_1 = 0 \text{ (or } \pi) \qquad \vartheta_2 = \vartheta_3 = \theta \qquad \text{and} \qquad \phi_2 = 0 \qquad \phi_3 = \pi$$

and for the collinear configuration

$$\vartheta_1 = \theta_{\mathrm{a}} \qquad \vartheta_2 = \vartheta_3 = \theta_{\mathrm{b}} \qquad \text{and} \qquad \phi_1 = \pi \qquad \phi_2 = \phi_3 = 0.$$

The evaluation of (A2) is tedious but straightforward. One obtains the sum of two contributions:

$$\begin{aligned} F_{\mathrm{m}}^2 &= S^2 f \sum_\tau \{I_1 \delta(\boldsymbol{k} - \boldsymbol{\tau}) + I_2[\delta(\boldsymbol{k} + \boldsymbol{Q} - \boldsymbol{\tau}) + \delta(\boldsymbol{k} - \boldsymbol{Q} - \boldsymbol{\tau})]\} \\ f &= (2\pi)^3 N_{\mathrm{m}}/V_{0\mathrm{m}} \end{aligned} \tag{A4}$$

where τ is a reciprocal lattice vector, N_m and V_{0m} are number and volume of the magnetic unit cells.

We give the results for the 'umbrella', the coplanar and the collinear configurations.

For the 'umbrella' there is a magnetic contribution to the nuclear reflection intensity proportional to $I_1 = I_{1,\mathrm{umb}}$

$$I_{1,\mathrm{umb}} = (1 - \tilde{k}_z^2)\cos^2\theta\{3 + 2\cos(\boldsymbol{k}\cdot\boldsymbol{d}_2) + 2\cos(\boldsymbol{k}\cdot\boldsymbol{d}_3) + 2\cos[\boldsymbol{k}\cdot(\boldsymbol{d}_2 - \boldsymbol{d}_3)]\} \tag{A5}$$

and the 'satellite' intensity $I_2 = I_{2,\mathrm{umb}}$

$$I_{2,\mathrm{umb}} = \tfrac{1}{4}(1 + \tilde{k}_z^2)\sin^2\theta\{3 - \cos(\boldsymbol{k}\cdot\boldsymbol{d}_2) - \cos(\boldsymbol{k}\cdot\boldsymbol{d}_3) - \cos[\boldsymbol{k}\cdot(\boldsymbol{d}_2 - \boldsymbol{d}_3)]\}. \tag{A6}$$

For the coplanar configurations with $\boldsymbol{S}_1 = (0, 0, \pm 1)$ one finds for the intensity at $(n/3, n/3, l)$

$$I_{1,\mathrm{cop}} = (1 - \tilde{k}_z^2)\{1 + 2\cos^2\theta[1 + \cos(\boldsymbol{k}\cdot\boldsymbol{d}_2)] \pm 2\cos\theta[\cos(\boldsymbol{k}\cdot\boldsymbol{d}_2) + \cos(\boldsymbol{k}\cdot\boldsymbol{d}_3)]\} \tag{A7}$$

and for the 'satellite'

$$I_{2,\mathrm{cop}} = \tfrac{1}{2}(1 + \tilde{k}_z^2)\sin^2\theta[1 - \cos(\boldsymbol{k}\cdot\boldsymbol{d}_2)]. \tag{A8}$$

Remember that for these two configurations ($\pm$) two different functions of h for $\cos\theta$ have to be used (see table 1).

For the collinear configuration

$$\begin{aligned} I_{1,\mathrm{col}} = (1 - \tilde{k}_z^2)[\![&\cos^2\theta_\mathrm{a} + 2\cos^2\theta_\mathrm{b}\{1 + \cos[\boldsymbol{k}\cdot(\boldsymbol{d}_2 - \boldsymbol{d}_3)]\} \\ &+ 2\cos\theta_\mathrm{a}\cos\theta_\mathrm{b}[\cos(\boldsymbol{k}\cdot\boldsymbol{d}_2) + \cos(\boldsymbol{k}\cdot\boldsymbol{d})_3)]]\!] \end{aligned} \tag{A9}$$

and

$$\begin{aligned} I_{2,\mathrm{col}} = \tfrac{1}{4}(1 + \tilde{k}_z^2)[\![&\sin^2\theta_\mathrm{a} - 2\sin\theta_\mathrm{a}\sin\theta_\mathrm{b}[\cos(\boldsymbol{k}\cdot\boldsymbol{d}_2) + \cos(\boldsymbol{k}\cdot\boldsymbol{d}_3)] \\ &+ 2\sin^2\theta_\mathrm{b}\{1 + \cos[\boldsymbol{k}\cdot(\boldsymbol{d}_3 - \boldsymbol{d}_2)]\}]\!]. \end{aligned} \tag{A10}$$

In the main part of the paper, to conform with the notation in the paper of Adachi *et al* (1980), we use reciprocal lattice vectors for the chemical unit cell. The reflection indices (hhl) for the magnetic unit cell then transform to $(h/3, h/3, l)$ for the chemical unit cell.

For peaks at reciprocal lattice points of type (hhl),

$$\cos(\boldsymbol{k}\cdot\boldsymbol{d}_i) = 1 \tag{A11}$$

and for those like $(h \pm \frac{1}{3}, h \pm \frac{1}{3}, 1)$ and $(h \pm \frac{1}{3}, h \pm \frac{1}{3}, l \pm \delta)$

$$\cos(\boldsymbol{k}\cdot\boldsymbol{d}_i) = -1/2 \tag{A12}$$

have to be inserted in (A5) to (A10) to obtain expressions that depend only on the typical configuration angles in the applied field and on the z component of the normalized scattering vector. Using table 1, one obtains the expressions (9) to (14).

References

Adachi K, Achiwa N and Mekata M 1980 *J. Phys. Soc. Japan* **49** 545

Chubukov A V and Golosov D I 1991 *J. Phys.: Condens. Matter* **3** 69

Fedoseeva N V, Gekht R S, Velikanova T A and Balaev A D 1985 *JETP Lett.* **41** 406

Gekht R S, Fedoseeva N V, Dolina V A and Balaev A D 1989 *Phys. Status Solidi* b **155** 639

Jacobs A E, Nikuni T and Shiba H 1993 to be published

Kawamura H 1984 *J. Phys. Soc. Japan* **53** 2452

—— 1991 *J. Phys. Soc. Japan* **61** 1299

LeDang K, Veillet P and Renard J P 1977 *Solid State Commun.* **24** 313

Mekata M, Ajiro Y, Sugino T, Oohara A, Ohara K, Yasuda S, Oohara Y and Yoshizawa H 1994 *Proc. Int. Conf. on Magnetism (Warsaw, 1994); J. Magn. Magn. Mater.* at press

Mino M, Ubukata K, Bokui T, Arai M, Tanaka H and Motokawa M 1993 *Proc. 5th Int. Symp. on Advanced Nuclear Energy Research (Mito, Japan, March 1993)* to be published

Miyashita S 1986 *Prog. Theor. Phys., Suppl.* **87** 112

Nikuni T and Shiba H 1993 *J. Phys. Soc. Japan* **62** 3268

Nojiri H, Tokunaga Y and Motokawa M 1988 *J. Physique* **49** Suppl.C8, 1459

Ohta H, Imagawa S, Motokawa M and Tanaka H 1993 *J. Phys. Soc. Japan* **62** 3011

—— 1994 *Proc. FHMF '93; Physica* B at press

Palme W, Kriegelstein H, Gojkovic G and Lüthi B 1993 *Int. J. Mod. Phys.* B **7** 1013

Palme W, Mertens F, Born O, Lüthi B and Schotte U 1990 *Solid State Commun.* **76** 873

Plumer M L and Caillé A 1990 *Phys. Rev.* B **42** 10388

Rastelli E and Tassi A 1994 *Phys. Rev.* B **49** 9679

Schlueter A W, Jacobson R A and Rundle R E 1966 *Inorg. Chem.* **25** 277

Tanaka H, Schotte U and Schotte K-D 1992 *J. Phys. Soc. Japan* **61** 1344

Tazuke Y, Tanaka H, Iio K and Nagata K 1981 *J. Phys. Soc. Japan* **50** 3919